Available online at www.sciencedirect.com
SCIENCE DIRECT®
Journal of Solid State Chemistry 178 (2005) 2880–2896
JOURNAL OF SOLID STATE CHEMISTRY
www.elsevier.com/locate/jssc

L-lysine-L-tartaric acid: New molecular complex with nonlinear optical properties. Structure, vibrational spectra and phase transitions

S. Debrus[a], M.K. Marchewka[b,*], J. Baran[b], M. Drozd[b], R. Czopnik[b], A. Pietraszko[b], H. Ratajczak[b]

[a]*Laboratoire d'Optique des Solides, UMR CNRS 7601, Université Pierre et Marie Curie (Paris 6), Campus Boucicaut, Case 80, Bureau 11-1-3, 140, rue de Lourmel 75015, Paris, France*
[b]*Institute of Low Temperature and Structure Research, Polish Academy of Sciences, Okólna 2, 50-950 Wrocław, Poland*

Received 6 November 2004; received in revised form 3 June 2005; accepted 6 June 2005

Abstract

The first X-ray diffraction and vibrational spectroscopic analysis of a novel complex between L-lysine and L-tartaric acid is reported. The structure was solved in two temperatures (320 and 260 K) showing incommensurate phase between them. Room-temperature powder infrared and Raman measurements for the L-lysine-L-tartaric acid molecular complex (1:1) were carried out. DSC measurements on powder samples indicate two phase transitions points at about 295, 300 and 293, 300 K, for heating and cooling, respectively, with noticeable temperature interval between them. Second harmonic generation efficiency $d_{eff} = 0.35\ d_{eff}$ (KDP).

Keywords: Lysine; Tartrates; Hydrogen bond; Phase transitions; FTRaman; FTIR; Structure–spectra correlation; Incommensurate phase; Second harmonic generation

1. Introduction

L-lysine-L-tartaric acid [$(N_2H_{14}C_6O_2)$–$(C_4H_6O_6)$] compound has been chosen for study as a potential material for nonlinear optics because of its non-centrosymmetric structure in the wide temperature range [1]. The tartaric acid forms a broad family of hydrogen-bonded crystals. As the investigated compound belongs to the family of cation-tartaric acid compounds, like many of them, it can undergo ferroelectric phase transition.

The structure of tartaric acid is known [2,3]. The results obtained during the analysis of the tartrates structure can be used to discuss a design strategy for the engineering of crystals with predesigned architecture [4,5]. The salts of tartaric acid were intensively studied by means of structural [6–18], spectroscopic [19–23], optical [24–28] and dielectric [29,30] methods.

Some tartrates exhibit structural phase transitions, e.g. [31,32], and in many cases [33–38] vibrational spectroscopy was effectively used to study them. In lithium the thallium tartrate monohydrate crystal a soft-mode behaviour at high pressure was discovered by Kamba et al. [39,40]. Vibrational circular dichroism (VCD) spectra were analysed to understand the optical activity of tartrates [24].

An infrared spectroscopy is an excellent tool for the investigation of the hydrogen bonds. Thus, the vibrational spectra can be helpful in the elucidation of the role of such a kind of interaction in the structure of the crystals exhibiting nonlinear optical properties. The influence of the strong and very strong hydrogen bonds on the non-linear optical properties of the crystal was already considered [41].

*Corresponding author. Polska Akademia Nauk, Wodzimierz Trzebiatowski Instytut Niskich Temperatur i Badan Strukturalnych, Zaklad Spektroskopii Molekularnej, ul. Okolna 2 (V 117)-skr. poczt.1410, PL-50-422 Wroclaw 2, Poland. Fax: +48 71 344 10 29.
E-mail address: mkm@int.pan.wroc.pl (M.K. Marchewka).

0022-4596/$ - see front matter © 2005 Elsevier Inc. All rights reserved.
doi:10.1016/j.jssc.2005.06.029

Some novel non-linear optical (NLO) crystals of non-centrosymmetric structures based on hydrogen bond interactions, namely 3-nitrobenzoic acid hydrazide [42] and the complex of orthoarsenic acid with NH_2-C $(CH_2OH)_3$ [43], have been discovered recently.

The role of tartaric acid molecule in the NLO activity of the crystal was also studied in [44,45]. In this context it is also worthwhile mentioning the complex of 2-amino-5-nitro-pyridine with tartaric acid [46], in which a second harmonic generation was observed, as well as a number of salts of substituted pyridines with L-tartaric acid exhibiting non-linear optical behaviour [47].

Some computation of the first hyperpolarizability, β, for hydrogen-bonded salts and acid–base pair, which has a crucial importance for the classification of material as having potential application for second harmonic generation, was done by Blagden et al. [48]. Finally, it seems worthwhile mentioning that a weak ferromagnetism has been discovered quite recently [49] in manganese tartrate dihydrate.

2. Experimental

Preparation: The L-lysine (Aldrich, 99%) and L-tartaric acid (Aldrich, 99%) were used as supplied. Good quality single-crystalline material was grown from aqueous solution containing the components in molar ratio (1:1). The solution slowly evaporated at room temperature.

X-ray *data collection*: The unit cell dimensions and intensity data were obtained with a KUMA Diffraction KM4/CCD single-crystal diffractometer. Data collection for the purpose of structure determination was performed at 320, 298 and 260 K.

The sample was selected under polarising microscope and examined by means of oscillation method. The intensity data were collected with graphite-monochromated Mo$K\alpha$ radiation in the ω-scan mode with the scan step $\Delta\omega = 0.75^\circ$ for one image. A total of 1060 images of six sets of exposures with different orientations in the reciprocal space were recorded. One image was monitored as a standard after every 40 images. The lattice parameters were calculated by using about 120 reflections obtained from 30 images of different orientations. For the structure solution and refinement the lattice parameters were then refined for all collected reflections. Integrated intensities were corrected for Lorentz polarisation and absorption effects by using KUMA Diffraction KM4/CCD Software [50]. The crystal data and other experimental details are given in Table 1. The temperature conditions at 320 K were controlled and maintained using CPC511 Oxford Cryosystem Cooler with cold nitrogen gas stream to an accuracy of ± 0.5 K.

Structure solution and refinement: The structure was solved by a direct method and subsequent difference Fourier syntheses of SHELXTL_PLUS program system [51] and the structure refinement was done by using SHELXL97 [52] and JANA2000 [56]. Anisotropic thermal displacement parameters' refinement was used for all non-hydrogen atoms at phase III. In high-temperature phase I and incommensurate phase II anisotropic displacement parameters were refined only for non-hydrogen atoms of tartaric acid molecule.

Spectroscopic measurements: The vibrational measurements were carried out at room temperature. Infrared spectra were taken with a Bruker IFS-88 spectrometer in the region of 4000–80 cm^{-1}. The resolution was set up to 2 $cm^{-1}$and signal/noise ratio was established by 32 scans, weak apodisation. Powder Fourier Transform Raman (FTRaman) spectra were taken with an FRA-106 attachment to the Bruker IFS-88 spectrometer equipped with a Ge detector cooled to liquid nitrogen temperature. Nd^{3+}:YAG air-cooled diode pumped laser of power ca. 200 mW was used as an exciting source. The incident laser excitation was 1064 nm. The scattered light was collected at the angle of 180° in the region of 3600–80 cm^{-1}, resolution 2 cm^{-1}, 256 scans. Due to the poor detector response, the Raman counterparts of the infrared bands located above 3200 cm^{-1} are not observed in the spectra presented in Figs. 10 and 11.

The polycrystalline powders were achieved by grinding in agate mortar with a pestle. Samples, as suspensions in oil, were put between KBr wafers. The powder infrared spectra were taken in Nujol and Fluorolube© emulsions to eliminate the bands originating from used oils.

Differential scanning calorimetry measurements: DSC was carried out on a Perkin Elmer DSC-7 calorimeter equipped with a CCA-7 low-temperature attachment with a heating/cooling rate of 20 K/min. The sample of the mass ca. 26 mg was sealed in the aluminium caps.

Second harmonic generation: SHG experiment was carried out using the Kurtz–Perry powder technique described in [53]. The calibrated samples (studied and KDP) were irradiated at 1064 nm by a Quanta Ray DCR-11 Nd^{+}:YAG laser and the second harmonic beam power diffused by the powder sample (at 532 nm) was measured as a function of the fundamental beam power.

3. Results and discussion

The crystal structure: In order to investigate the relationship of the spectral and nonlinear optical properties to the symmetry and structure, an X-ray structure investigation of the L-lysine-L-tartaric acid complex was undertaken.

Table 1
Experimental and refinement details for L-lysine L-tartaric acid compound

Structure at temperature	260 K	298 K	320 K
Phase	III	II	I
Empirical formula	$C_{10}H_{20}N_2O_8$	$C_{10}H_{20}N_2O_8$	$C_{10}H_{20}N_2O_8$
Cell setting	Monoclinic	Monoclinic	Monoclinic
(Super)space group	$P2_1$	$P2_1(\alpha 0 \gamma)$	$P2_1$
a (Å)	5.124(1)	5.103(1)	5.104(1)
b (Å)	17.385(3)	17.445(2)	17.525(3)
c (Å)	22.400(4)	7.538(1)	7.588(1)
β (deg)	95.08(3)	97.94(1)	97.60(2)
Modulation wavevector	—	(0.0159(5), 0, 0.2829(7))	—
V (Å^3)	1987.6(6)	664.6	672.80
Formula units	6	2	2
Molecular weight	296.28	296.28	296.28
Calculated density (Mg m^{-3})	1.485	1.480	1.462
Data collection			
Diffractometer		KUMA CCD	
Radiation type		Mo $K\alpha$	
Wavelength		0.71073	
Absorption correction type	None	None	None
μ (mm^{-1})	0.129	0.128	0.127
Range of:			
H	$-6 \rightarrow 6$	$-6 \rightarrow 5$	$-6 \rightarrow 7$
K	$-22 \rightarrow 22$	$-23 \rightarrow 22$	$-23 \rightarrow 23$
L	$-29 \rightarrow 28$	$-10 \rightarrow 10$	$-9 \rightarrow 10$
M	—	$-1 \rightarrow 1$	—
Criterion for observed reflections	$I > 2\sigma(I)$	$I > 3\sigma(I)$	$I > 3\sigma(I)$
No. of reflections (obs, all)			
Measured	18,690	9656, 19295	3835, 6397
Unique	9290, 4169	4834, 9685	1870, 3294
Main	—	2279, 3228	—
First-order satellites	—	2555, 6457	—
R_{int}(obs): all, main, satellites	6.84	2.60, 1.87, 7.04	5.12
Refinement			
Refinement on	F^2	F	F
Program used	Shelxl97	Jana2000	Jana2000
Weighting scheme	$w = 1/[\sigma^2(F_0^2) + (0.0250P)^2 + 0.0250P]$ where $P = (F_o^2 + 2F_c^2)/3$		
$w = [\sigma^2(F) + (0.02F)^2]^{-1}$			
$w = [\sigma^2(F) + (0.02F)^2]^{-1}$			
Extinction correction	Shelxl97	None	None
Extinction coefficient	0.00647(15)	—	—
S_{obs}, S_{all}	0.932	3.07, 2.34	2.14, 1.77
R_{obs}, wR_{obs}			
All reflections	5.25, 9.19	9.43, 11.68	5.97, 6.76
Main reflections	—	6.84, 8.44	—
First-order satellites	—	14.55, 16.05	—
R_{all}, wR_{all}			
All reflections	10.78, 10.55	14.64, 12.64	9.24, 7.52
Main reflections	—	8.80, 8.90	—
First-order satellites	—	22.48, 17.48	—
No. of parameters	782	211	171
$(\Delta/\text{s.u.})_{max}$	1.597	0.012	0.001
$\Delta\rho_{max}$ (eÅ^{-3})	0.294	0.77	0.30
$\Delta\rho_{min}$ (eÅ^{-3})	−0.241	−0.56	−0.21

Details of data collection and refinement for all the phases are given in Table 1. Fractional atomic coordinates and equivalent isotropic displacements parameters of phases I, II and III are presented in Tables 2, 5 and 9, respectively. Anisotropic displacement parameters are presented in Tables 3, 6 and 10, and

selected bond distances and angles in Tables 4 and 7. Amplitudes of displacive and occupation modulation waves of the incommensurate structure of phase II are presented in Table 8 (see Tables 2–10).

Atom numbering scheme, molecular arrangement and projections of the studied structure are depicted in Figs. 1–9.

The structure solution and refinement of the crystal at a temperature range of 320–260 K indicate that all crystal phases have monoclinic $P2_1$ symmetry. Also, the molecule arrangement does not change generally with temperature change. The crystal structure at studied temperatures consists of the tartaric acid and lysine molecule layers stacked perpendicularly to [010]. Nevertheless, slight changes in molecular structure are observed during the phase transitions.

There are three independent molecules of both tartaric acid and lysine molecules at low-temperature phase III (below 296 K). They differ from each other in conformation, but it seems that modulation—commensurate (phase III) and incommensurate (phase II)—is caused by conformation change of lysine chains and displacive modulation of tartaric acid molecules. It is supposed that chains start to vibrate without restraints and an enormous enlargement of thermal displacement parameters of carbon atoms is observed with temperature increase. This leads to the disappearance of the modulation and is an origin of phase I with disordered lysine molecules. In this paper solution of the disordered structure of phase I and incommensurate structure of phase II required refinement of the atomic positions which lay very close to each other. For this reason only isotropic displacement parameters were used in the refinement of these phases. See Figs. 1 and 2 and Tables 2 and 5 for details.

Due to the low diffraction power of X-ray in H-atom detection, the existence of COO^- or COOH in the crystal was deduced on the basis of carboxylic group geometry. Comparison of the C–O bonds with the standard values [54] shows that some of the carboxylic groups are ionised. This fact implicates an appearance of NH_3^+ group in lysine molecules. Also, when both

Table 2
Fractional atomic coordinates and equivalent isotropic displacement parameters at 320 K

Atom	x	y	z	U_{iso} (Å^2)
Tartaric acid				
C1	0.3299(6)	0.1556(12)	0.0261(4)	0.0373(9)
C2	0.2517(5)	0.1441(12)	0.2113(3)	0.0368(10)
C3	0.2691(7)	0.2211(12)	0.3074(4)	0.0446(11)
C4	0.1697(7)	0.2153(12)	0.4867(4)	0.0468(12)
O1	0.5659(4)	0.1668(12)	0.0127(3)	0.0485(8)
O2	0.1453(4)	0.1548(12)	−0.1053(3)	0.0444(7)
O3	0.0034(4)	0.1088(12)	0.2155(3)	0.0450(7)
O4	0.1204(6)	0.2775(12)	0.2030(3)	0.0605(9)
O5	0.3167(5)	0.1708(12)	0.5972(3)	0.0659(10)
O6	−0.0298(6)	0.2468(12)	0.5193(3)	0.0747(12)
H2	0.367	0.104	0.2752	0.044118
H3	0.456	0.2397	0.3223	0.053535
H32	−0.1379	0.1407	0.1481	0.04525
H42	−0.0635	0.2604	0.1754	0.058915
H53	0.2392	0.1662	0.7092	0.063728
Lysine 1				
C12	0.1957(14)	−0.1240(13)	0.1397(9)	0.0334(17)
C11	0.3795(19)	−0.0905(14)	0.0131(13)	0.037(3)
N21	0.2550(14)	−0.2118(13)	0.1760(10)	0.049(2)
C14	0.536(2)	−0.0742(13)	0.4057(13)	0.069(3)
C13	0.2403(12)	−0.0814(13)	0.3214(8)	0.0417(15)
C16	0.8094(16)	−0.0138(13)	0.6680(10)	0.0557(19)
C15	0.5353(16)	−0.0278(13)	0.5803(9)	0.0504(16)
N12	0.8351(16)	0.0177(13)	0.8609(11)	0.046(2)
O11	0.5528(13)	−0.1384(13)	−0.0287(9)	0.055(2)
O12	0.3143(14)	−0.0337(13)	−0.0553(10)	0.056(2)
H131	0.1368	−0.1072	0.4074	0.050038
H132	0.1591	−0.0295	0.3074	0.050038
H141	0.6369	−0.0456	0.3227	0.082385
H142	0.6101	−0.1262	0.4345	0.082385
H151	0.4343	−0.0564	0.6633	0.060501
H152	0.4442	0.0221	0.5529	0.060501
H161	0.9021	0.0212	0.5925	0.066877
H162	0.9152	−0.0618	0.6662	0.066877
H121	1.0107	0.0028	0.9263	0.054662
H122	0.8202	0.0746	0.8574	0.054662
H123	0.691	−0.004	0.9231	0.054662
H111	0.042	−0.2267	0.043	0.049382
H112	0.3535	−0.2316	0.1257	0.049382
H113	0.1267	−0.2265	0.2582	0.049382
H12	0.0071	−0.116	0.0884	0.040132
H22	0.0787	−0.1042	0.1758	0.050477
H211	0.4384	−0.231	0.2136	0.058999
H212	0.1334	−0.2331	0.2566	0.058999
H213	0.1945	−0.2282	0.0511	0.058999
H221	0.6535	0.0644	0.8821	0.053108
H222	0.7706	−0.0223	0.8854	0.053108
H223	0.9696	0.0504	0.8812	0.053108

Table 2 (*continued*)

Atom	x	y	z	U_{iso} (Å^2)
Lysine 2				
N22	0.7887(16)	0.0305(13)	0.8386(11)	0.044(2)
O21	0.6055(13)	−0.1350(13)	0.0156(9)	0.0512(19)
O22	0.3576(14)	−0.0286(13)	−0.0135(10)	0.054(2)
C25	0.688(2)	−0.0503(14)	0.5957(13)	0.080(3)
C26	0.7504(16)	0.0290(13)	0.6533(10)	0.0591(19)
C23	0.4229(17)	−0.1265(13)	0.3597(11)	0.067(2)
N11	0.1780(14)	−0.2093(13)	0.1418(9)	0.0412(17)
C22	0.2533(15)	−0.1309(13)	0.1858(10)	0.042(2)
C21	0.3989(19)	−0.1028(13)	0.0398(13)	0.040(3)
C24	0.5095(19)	−0.0478(13)	0.4041(13)	0.057(3)
H231	0.5812	−0.1599	0.3575	0.079964
H232	0.324	−0.1468	0.4548	0.079964
H241	0.3513	−0.0148	0.4108	0.068918
H242	0.6184	−0.0287	0.3131	0.068918
H251	0.8551	−0.0786	0.586	0.096237
H252	0.5863	−0.0758	0.6834	0.096237
H261	0.5994	0.0631	0.6082	0.070917
H262	0.9161	0.0457	0.6075	0.070917

Table 3
Anisotropic displacement parameters (Å^2) at 320 K

Atom	U^{11}	U^{22}	U^{33}	U^{12}	U^{13}	U^{23}
C1	0.0391(16)	0.0442(17)	0.0301(14)	0.0035(15)	0.0098(12)	0.0013(13)
C2	0.0276(14)	0.054(2)	0.0304(15)	0.0026(13)	0.0089(11)	0.0055(13)
C3	0.047(2)	0.054(2)	0.0339(16)	−0.0071(16)	0.0105(14)	−0.0015(14)
C4	0.052(2)	0.056(2)	0.0345(17)	−0.0027(17)	0.0121(15)	−0.0003(15)
O1	0.0278(10)	0.0758(16)	0.0443(12)	0.0008(12)	0.0137(9)	0.0080(11)
O2	0.0371(11)	0.0682(15)	0.0284(10)	−0.0020(12)	0.0065(9)	0.0057(11)
O3	0.0400(12)	0.0539(13)	0.0431(12)	−0.0053(10)	0.0127(10)	0.0076(10)
O4	0.0830(19)	0.0547(16)	0.0442(13)	0.0099(14)	0.0102(12)	0.0022(11)
O5	0.0545(14)	0.109(2)	0.0364(13)	0.0115(17)	0.0144(11)	0.0125(14)
O6	0.090(2)	0.088(2)	0.0537(16)	0.0298(17)	0.0364(15)	0.0048(13)

Table 4
Selected bond distances and angles at 320 K

Atoms	
Tartaric acid	
C1–C2	1.524(6)
C2–C3	1.53(3)
C3–C4	1.517(5)
C1–O1	1.238(6)
C1–O2	1.278(3)
C2–O3	1.414(14)
C3–O4	1.42(2)
C4–O5	1.306(18)
C4–O6	1.212(14)
C2–C1–O1	118.2(3)
C2–C1–O2	117.5(4)
O1–C1–O2	124.2(4)
C1–C2–C3	108.5(14)
C1–C2–O3	115.1(6)
C3–C2–O3	111.7(9)
C2–C3–C4	111.3(14)
C2–C3–O4	110.8(7)
C4–C3–O4	109.2(10)
C3–C4–O5	112.6(9)
C3–4–O6	122.8(11)
O5–C4–O6	124.6(6)
Lysine 1	
C11–O11	1.29(2)
C11–O12	1.15(3)
N11–C12	1.50(3)
C12–C13	1.558(17)
C14–C13	1.564(12)
C14–C15	1.55(2)
C16–C15	1.488(12)
C16–N12	1.554(16)
C22–C21	1.497(17)
C22–N21	1.42(3)
N11–C12–C11	115.4(13)
N11–C12–C13	118.1(11)
C11–C12–C13	109.7(13)
C12–C11–O11	113.4(19)
C12–C11–O12	116.5(12)
O11–C11–O12	128.2(12)
C13–C14–C15	106.3(10)
C15–C16–N12	115.9(8)
C14–C15–C16	111.1(9)

Table 4 (*continued*)

Atoms	
Lysine 2	
O21–C21	1.231(18)
O22–C21	1.37(3)
C25–C26	1.48(3)
C25–C24	1.610(13)
C23–C22	1.481(11)
C23–C24	1.47(3)
N22–C26	1.393(11)
C23–C22–C21	110.7(9)
C23–C22–N21	95.2(13)
O21–C21–O22	119.5(15)
O21–C21–C22	118.6(17)
O22–C21–C22	117.2(14)
C25–C24–C23	107.3(15)
C26–C25–C24	108.4(15)
N22–C26–C25	108.2(16)
C22–C23–C24	112.0(16)

COO^- and COOH groups coexist in the crystal, it is key to annihilation of a possible centre of inversion [45].

As was also shown by Row [45], the multidirectional hydrogen-bonded tartrate anions provide a conformational rigid environment for the incorporation of cations to form acentric crystalline salts—SHG materials. Also the L-lysine-L-tartaric acid complex belongs to these crystals family.

The tartaric acid molecules are bonded into a layer by O···O-type hydrogen bonds of length ~2.5 and ~2.7 Å to generate a two-dimensional framework (Table 11). The lysine molecules layers are maintained by O···N-type bonds of ~2.8 Å length. These two types of layers are joined together by both types of hydrogen bonds of ~2.8 Å length to result in a stable, 3D aggregate.

Taking into account the classification proposed in [45], the L-lysine-L-tartaric acid complex has got a Type I structure where infinite layers or chains motifs are parallel. It is also characterised by a conformationally rigid framework structure with conserved interlayer

Table 5
Fractional atomic coordinates and equivalent isotropic displacement parameters at 298 K

Atom	x	y	z	U_{iso} (Å^2)
Tartaric acid				
C1	0.3303(5)	0.1527(9)	0.0186(3)	0.0260(8)
C2	0.2535(5)	0.1425(9)	0.2067(3)	0.0273(9)
C3	0.2721(6)	0.2207(9)	0.3021(4)	0.0337(10)
C4	0.1725(7)	0.2141(9)	0.4806(4)	0.0350(10)
O1	0.5649(4)	0.1641(9)	0.0059(3)	0.0380(7)
O2	0.1458(4)	0.1531(9)	−0.1109(2)	0.0351(7)
O3	0.0055(4)	0.1074(9)	0.2116(3)	0.0340(7)
O4	0.1281(6)	0.2767(9)	0.1959(3)	0.0489(9)
O5	0.3204(5)	0.1707(9)	0.5945(3)	0.0527(9)
O6	−0.0274(6)	0.2454(9)	0.5119(3)	0.0596(11)
H2	0.3685	0.1024	0.2726	0.032725
H3	0.4572	0.2409	0.3185	0.040436
H32	−0.1379	0.1407	0.1481	0.04525
H42	−0.0635	0.2604	0.1754	0.058915
H53	0.2392	0.1662	0.7092	0.063728
Lysine 1				
C12	0.1856(12)	−0.1235(10)	0.1382(7)	0.0213(10)
C11	0.3670(12)	−0.0959(10)	0.0052(7)	0.0175(9)
N11	0.2323(16)	−0.2076(10)	0.1724(8)	0.0298(10)
C14	0.5219(11)	−0.0708(10)	0.3992(7)	0.0249(10)
C13	0.2330(11)	−0.0790(10)	0.3165(7)	0.0221(10)
C16	0.8104(13)	−0.0196(10)	0.6723(7)	0.0245(11)
C15	0.5343(13)	−0.0306(10)	0.5838(7)	0.0333(12)
N12	0.8186(14)	0.0157(10)	0.8609(7)	0.0230(10)
O11	0.5574(11)	−0.1358(10)	−0.0169(7)	0.0292(9)
O12	0.3130(12)	−0.0312(10)	−0.0578(6)	0.0272(8)
H12	−0.0025	−0.1154	0.0839	0.025568
H131	0.1304	−0.1036	0.4051	0.026492
H132	0.1502	−0.0271	0.2998	0.026492
H141	0.6185	−0.0391	0.3185	0.029865
H142	0.6048	−0.1227	0.4157	0.029865
H151	0.4337	−0.0615	0.6634	0.039993
H152	0.4437	0.0203	0.568	0.039993
H161	0.9072	0.0145	0.5968	0.029342
H162	0.9041	−0.0701	0.6818	0.029342
H111	0.1621	−0.2373	0.0626	0.035735
H112	0.4264	−0.2173	0.203	0.035735
H113	0.1394	−0.2242	0.2744	0.035735
H121	0.9955	0.0057	0.9323	0.027573
H122	0.7885	0.0722	0.85	0.027573
H123	0.6773	−0.008	0.9226	0.027573
Lysine 2				
N22	0.775(2)	0.0273(11)	0.8229(11)	0.0557(15)
O21	0.5957(18)	−0.1416(11)	0.0165(11)	0.0660(15)
O22	0.373(2)	−0.0316(11)	−0.0025(10)	0.0689(15)
C25	0.724(2)	−0.0406(11)	0.5292(14)	0.108(3)
C26	0.774(2)	0.0317(11)	0.6296(12)	0.071(2)
C23	0.3799(19)	−0.1307(10)	0.3716(12)	0.0641(19)
N21	0.1713(19)	−0.2128(10)	0.1337(11)	0.0376(13)
C22	0.2340(16)	−0.1316(10)	0.1794(11)	0.0380(14)
C21	0.4081(18)	−0.0986(11)	0.0536(11)	0.0473(16)
C24	0.459(2)	−0.0513(11)	0.4414(13)	0.097(3)
H22	0.0671	−0.1008	0.166	0.045551
H231	0.5405	−0.164	0.3789	0.076884
H232	0.2672	−0.1557	0.4535	0.076884
H241	0.3314	−0.0331	0.5214	0.116891
H242	0.4211	−0.0131	0.3422	0.116891
H251	0.8508	−0.0452	0.4396	0.12949
H252	0.7754	−0.0849	0.6109	0.12949
H261	0.644	0.0713	0.578	0.08566
H262	0.9449	0.0544	0.6039	0.08566
H211	0.1903	−0.2441	0.2458	0.045078
H212	−0.0145	−0.2166	0.0717	0.045078
H213	0.2959	−0.2324	0.0527	0.045078
H221	0.9609	0.0233	0.884	0.066799
H222	0.6907	0.0745	0.8651	0.066799
H223	0.6724	−0.0188	0.8522	0.066799

separation ca. 10 Å, and in our crystal the distance between tartaric acid layers exceeds 9 Å. In such a type of structure SHG is not high, which is in congruence with our SHG measurements.

3.1. Description of the incommensurate phase of L-lysine L-tartaric acid compound

Low-temperature phase: The structure of the low-temperature phase is crucial to the understanding of the modulation observed in the incommensurate phase. It is due to the fact that the superstructure appears when the period of the modulation waves becomes commensurate with the periodicity of the crystal lattice. Thus, the character of the modulation present in the incommensurate phase should be visible in the low-temperature three-fold superstructure, in which the modulation vector locks its value at 1/3 along the c direction. Consequently, the displacive waves existing in incommensurate phase lead to shifts in the corresponding positions in the superstructure, and the remains of the occupation waves are visible as the statistically occupied positions become independent.

Both these features are recognised in the superstructure of the low-temperature phase, in which there are three independent molecules for both lysine and tartaric acid. As lysine is considered, it is noticeable that the conformation of two of these molecules is the same, and the conformation of the third substantially differs. On the basis of this observation we presume that the lysine molecules are subjected to occupation modulation in the incommensurate phase, since two conformations of lysine occur both in the average structure of the incommensurate phase and in the disordered structure of the high-temperature phase.

The projection of the unit cell along [101] direction, Fig. 9, reveals that the positions of the three independent tartaric acid molecules do not coincide in the plane. The same feature is present for two molecules of lysine which have the same conformation. It suggests that displacive modulation is present in the incommensurate phase for both tartaric acid and lysine molecules. The reason for why we consider the projection along the

Table 6
Anisotropic displacement parameters (Å^2) at 298 K

Atom	U^{11}	U^{22}	U^{33}	U^{12}	U^{13}	U^{23}
C1	0.0287(15)	0.0278(15)	0.0228(12)	0.0028(13)	0.0076(11)	0.0021(12)
C2	0.0230(14)	0.0352(17)	0.0241(13)	0.0017(12)	0.0048(10)	0.0070(11)
C3	0.0339(17)	0.0407(19)	0.0271(15)	−0.0052(15)	0.0064(13)	0.0002(13)
C4	0.0396(19)	0.045(2)	0.0217(14)	−0.0052(16)	0.0089(13)	−0.0009(13)
O1	0.0241(11)	0.0587(15)	0.0326(10)	−0.0024(11)	0.0091(8)	0.0066(11)
O2	0.0295(11)	0.0560(14)	0.0199(9)	−0.0029(11)	0.0039(8)	0.0072(10)
O3	0.0296(11)	0.0426(13)	0.0303(10)	−0.0051(10)	0.0064(9)	0.0047(9)
O4	0.0635(17)	0.0433(15)	0.0400(13)	0.0047(13)	0.0077(11)	0.0031(10)
O5	0.0439(14)	0.090(2)	0.0266(11)	0.0093(15)	0.0113(10)	0.0087(13)
O6	0.0671(19)	0.079(2)	0.0378(14)	0.0251(15)	0.0252(13)	0.0074(12)

Table 7
Selected bond distances and angles at 298 K

Atoms	Average	Min.	Max.
Tartaric acid			
C1–C2	1.533(5)	1.532(5)	1.534(6)
C2–C1–O1	117.8(3)	117.8(3)	117.8(3)
C2–C1–O2	117.3(3)	117.3(3)	117.4(3)
C1–O1	1.230(6)	1.230(6)	1.230(5)
O1–C1–O2	124.8(4)	124.7(5)	124.8(4)
C1–O2	1.260(4)	1.260(4)	1.261(4)
C1–C2–C3	108.8(11)	108.8(11)	108.8(11)
C1–C2–O3	114.8(5)	114.8(4)	114.8(5)
C2–C3	1.54(2)	1.54(2)	1.54(2)
C3–C2–O3	111.7(7)	111.7(7)	111.8(7)
C2–O3	1.412(11)	1.412(11)	1.412(10)
C2–C3–C4	110.1(11)	110.1(11)	110.1(11)
C2–C3–O4	110.9(6)	110.9(6)	110.9(6)
C3–C4	1.508(5)	1.507(5)	1.508(6)
C4–C3–O4	110.3(8)	110.3(8)	110.4(8)
C3–O4	1.406(16)	1.405(16)	1.407(17)
C3–C4–O5	113.3(7)	113.3(7)	113.3(7)
C3–C4–O6	122.6(8)	122.5(8)	122.6(8)
C4–O5	1.306(14)	1.305(14)	1.307(15)
O5–C4–O6	124.1(5)	124.1(5)	124.1(5)
C4–O6	1.209(11)	1.208(11)	1.209(11)
Lysine 1			
C12–C11	1.534(13)	1.533(13)	1.534(14)
C11–C12–N11	108.9(11)	108.9(11)	108.9(11)
C11–C12–C13	112.1(11)	112.1(11)	112.1(11)
C12–N11	1.50(3)	1.50(3)	1.50(3)
N11–C12–C13	109.9(9)	109.9(9)	109.9(9)
C12–C13	1.543(15)	1.542(15)	1.543(15)
C12–C11–O11	118.1(14)	118.1(14)	118.1(14)
C12–C11–O12	114.5(11)	114.5(11)	114.5(11)
C11–O11	1.225(18)	1.225(18)	1.225(18)
O11–C11–O12	127.1(11)	127.1(11)	127.1(11)
C11–O12	1.24(2)	1.24(2)	1.24(2)
C14–C13	1.526(10)	1.526(10)	1.526(10)
C13–C14–C15	109.0(7)	109.0(7)	109.0(7)
C14–C15	1.553(14)	1.552(14)	1.553(14)
C12–C13–C14	115.4(8)	115.4(8)	115.4(8)
C16–C15	1.486(12)	1.486(12)	1.486(12)
C15–C16–N12	111.6(9)	111.6(9)	111.6(9)
C16–N12	1.545(15)	1.544(15)	1.546(16)
C14–C15–C16	112.3(8)	112.3(8)	112.3(8)

Table 7 (*continued*)

Atoms	Average	Min.	Max.
Lysine 2			
N22–C26	1.460(18)	1.459(18)	1.461(18)
O21–C21	1.28(2)	1.28(2)	1.28(2)
O22–C21	1.25(3)	1.25(3)	1.25(3)
C25–C26	1.48(3)	1.47(3)	1.48(3)
C26–C25–C24	115.7(16)	115.7(16)	115.7(16)
C25–C24	1.436(18)	1.433(18)	1.438(18)
N22–C26–C25	116.3(17)	116.2(17)	116.4(17)
C23–C22	1.536(15)	1.535(15)	1.538(15)
C22–C23–C24	114.0(14)	113.9(14)	114.1(14)
C23–C24	1.52(3)	1.52(3)	1.52(3)
N21–C22	1.48(3)	1.48(3)	1.49(3)
C23–C22–N21	106.8(14)	106.7(13)	106.8(14)
C23–C22–C21	109.9(10)	109.8(10)	109.9(10)
N21–C22–C21	110.4(13)	110.3(13)	110.5(13)
C22–C21	1.503(19)	1.500(19)	1.505(19)
O21–C21–O22	123.6(15)	123.6(15)	123.6(15)
O21–C21–C22	116.1(17)	116.1(17)	116.2(17)
O22–C21–C22	120.2(15)	120.2(15)	120.3(14)
C25–C24–C23	118.0(15)	117.9(15)	118.0(15)

[101] direction instead of the projection along the c direction is that the unit cell of the low-temperature phase III was chosen in slightly different way if compared to phases II and I. The [101] direction in the low-temperature phase III corresponds to the c direction in phases II and I.

The structure of the incommensurate phase: Observed main reflections satisfy the $k = 2n$ systematic extinction condition which indicates $P2_1$ space group for the average structure. Taking into account the measured modulation vector (0.015, 0, 0.28), the $P2_1(\alpha 0 \gamma)0$ superspace group was established unambiguously [57,58].

As the initial model of the average structure of the incommensurate phase the structure of the high-temperature phase was taken, in which some positions of atoms of disordered lysine molecules lay so close to

Table 8
Amplitudes of displacive and occupation modulation waves at 298 K

Molecule	Waves	x translation	y translation	z translation	ϕ rotation	χ rotation	ψ rotation	Occupancy
Tartaric acid								
	Sin	0.0085(2)	−0.00739(6)	−0.00072(17)	0.01000(10)	0.00017(3)	−0.00163(12)	—
	Cos	−0.0038(2)	0.00497(6)	0.00070(14)	0.00490(11)	0.00051(3)	−0.00128(11)	—
Lysine 1								
	Sin	0.0176(8)	−0.0013(2)	0.0256(5)	0.0069(4)	−0.00023(10)	0.0011(4)	0.69936
	Cos	−0.0128(7)	0.0040(2)	−0.0228(5)	−0.0032(3)	0.00030(9)	−0.0001(4)	0.585959
Lysine 2								
	Sin	−0.0041(12)	0.0014(4)	−0.0077(8)	0.0014(6)	−0.00212(18)	−0.0072(6)	−0.697094
	Cos	−0.0156(11)	0.0036(3)	−0.0251(7)	0.0034(5)	−0.00191(16)	−0.0058(5)	−0.59424

Table 9
Fractional atomic coordinates and equivalent isotropic displacement parameters at 260 K

Atom	x	y	z	U_{iso} (Å^2)
O1A	0.90817(12)	0.26521(4)	0.33517(3)	0.0338(2)
O2A	0.52373(12)	0.27394(4)	0.37363(3)	0.0373(2)
C1A	0.67005(19)	0.27708(5)	0.33055(4)	0.0280(3)
O3A	0.28111(12)	0.32654(4)	0.26836(3)	0.0363(2)
C2A	0.53181(18)	0.29338(5)	0.26819(4)	0.0269(3)
O4A	0.42084(14)	0.15767(4)	0.26582(3)	0.0435(2)
C3A	0.52875(19)	0.21812(6)	0.23271(4)	0.0317(3)
O5A	0.47669(13)	0.27237(4)	0.13600(3)	0.0453(2)
O6A	0.15315(14)	0.19797(4)	0.16261(3)	0.0563(3)
C4A	0.3652(2)	0.22786(6)	0.17378(5)	0.0346(3)
O1B	0.19150(13)	0.28687(4)	0.03753(3)	0.0351(2)
O2B	0.57008(12)	0.26654(4)	−0.00202(3)	0.0383(2)
C1B	0.32858(19)	0.27999(5)	−0.00632(4)	0.0292(3)
O3B	−0.06105(12)	0.31888(4)	−0.07281(3)	0.0356(2)
C2B	0.19067(18)	0.28485(5)	−0.07038(4)	0.0263(3)
O4B	0.07505(14)	0.14903(4)	−0.05821(3)	0.0414(2)
C3B	0.1810(2)	0.20304(6)	−0.09641(4)	0.0343(3)
O5B	0.12315(13)	0.24284(4)	−0.19763(3)	0.0460(3)
O6B	−0.20162(14)	0.17352(4)	−0.16382(3)	0.0480(3)
C4B	0.0087(2)	0.20431(6)	−0.15655(4)	0.0339(3)
O1C	0.76874(12)	0.75893(4)	0.33336(3)	0.0365(2)
O2C	1.15697(13)	0.76265(4)	0.29532(3)	0.0345(2)
C1C	1.01086(19)	0.76578(5)	0.33890(4)	0.0281(3)
O3C	1.39776(12)	0.81018(4)	0.40359(3)	0.0364(2)
C2C	1.1498(2)	0.77580(6)	0.40175(4)	0.0323(3)
O4C	1.28153(15)	0.64068(4)	0.39655(3)	0.0471(3)
C3C	1.1649(2)	0.69629(6)	0.43154(5)	0.0375(4)
O5C	1.51939(17)	0.66718(4)	0.50641(3)	0.0635(3)
O6C	1.20553(15)	0.74876(5)	0.52905(3)	0.0575(3)
C4C	1.3152(2)	0.70262(6)	0.49341(5)	0.0389(4)
O1D	0.90664(13)	0.56223(4)	0.32908(3)	0.0453(2)
O2D	0.68240(13)	0.45475(4)	0.34336(3)	0.0451(2)
C1D	0.70687(19)	0.52041(6)	0.32163(4)	0.0332(3)
C0D	0.48011(19)	0.54889(6)	0.27887(4)	0.0348(3)
N1D	0.50352(16)	0.63326(5)	0.27145(4)	0.0375(3)
C2D	0.46711(18)	0.50598(6)	0.21906(4)	0.0341(3)
C3D	0.7192(2)	0.50039(6)	0.18960(4)	0.0402(3)
C4D	0.6786(2)	0.46313(6)	0.12798(5)	0.0410(4)
C5D	0.9272(2)	0.45354(7)	0.09775(4)	0.0446(4)
N2D	0.86903(17)	0.41893(5)	0.03582(4)	0.0420(3)
O1E	−0.01040(13)	0.45571(4)	0.69326(3)	0.0467(2)
O2E	0.22179(13)	0.56239(4)	0.67923(3)	0.0477(2)
C1E	0.0230(2)	0.52107(6)	0.67017(4)	0.0345(3)

Table 9 (*continued*)

Atom	x	y	z	U_{iso} (Å^2)
C0E	−0.1986(2)	0.54804(6)	0.62559(5)	0.0387(4)
N1E	−0.17952(18)	0.63278(5)	0.61681(4)	0.0474(3)
C2E	−0.2159(2)	0.50151(7)	0.56894(5)	0.0563(4)
C3E	0.0441(2)	0.49290(7)	0.54024(5)	0.0526(4)
C4E	0.0076(2)	0.45433(8)	0.47984(5)	0.0612(4)
C5E	0.2481(2)	0.44141(9)	0.45034(5)	0.0716(5)
N2E	0.19583(16)	0.40591(5)	0.38899(4)	0.0404(3)
O1F	0.41045(13)	0.07221(4)	0.01828(3)	0.0507(3)
O2F	0.64541(14)	−0.03509(4)	0.01324(3)	0.0484(3)
C1F	0.61209(19)	0.03201(6)	0.03051(5)	0.0365(3)
C0F	0.82385(18)	0.06651(6)	0.07451(4)	0.0315(3)
N1F	0.85728(16)	0.14940(5)	0.05865(4)	0.0399(3)
C2F	0.7442(2)	0.06249(6)	0.13934(5)	0.0444(4)
C3F	0.7141(2)	−0.01992(6)	0.16266(5)	0.0450(4)
C4F	0.4360(2)	−0.04125(7)	0.17146(5)	0.0532(4)
C5F	0.4113(2)	−0.11760(6)	0.20417(5)	0.0491(4)
N2F	0.48594(17)	−0.10730(5)	0.27115(4)	0.0401(3)
H21C	0.9709(16)	0.6825(4)	0.4392(4)	0.025(2)
H21B	0.3127(16)	0.3119(5)	−0.1017(4)	0.039(3)
H21D	0.3333(13)	0.5303(4)	0.1940(3)	0.0058(19)
H22D	0.3868(15)	0.4503(5)	0.2267(3)	0.032(2)
H51E	0.1707(17)	0.3853(5)	0.4561(4)	0.043(3)
H31B	0.3581(18)	0.1919(5)	−0.1060(4)	0.044(3)
H31C	1.0368(17)	0.8112(5)	0.4299(4)	0.039(3)
H5A	0.376(2)	0.2783(6)	0.0978(4)	0.060(3)
H31A	0.6961(17)	0.2066(5)	0.2323(4)	0.035(3)
H71E	−0.2554(18)	0.6518(5)	0.6453(4)	0.044(3)
H81F	0.654(2)	−0.0836(6)	0.2777(5)	0.078(4)
H21A	0.6438(14)	0.3298(4)	0.2477(3)	0.018(2)
H01F	1.0326(18)	0.0398(5)	0.0708(4)	0.051(3)
H51F	0.2257(16)	−0.1368(5)	0.2044(4)	0.037(3)
H5B	0.003(3)	0.2570(7)	−0.2316(6)	0.115(5)
H81D	0.7127(17)	0.4363(5)	0.0192(4)	0.046(3)
H81E	0.038(2)	0.4216(6)	0.3702(5)	0.085(4)
H32F	0.817(2)	−0.0541(7)	0.1334(5)	0.089(4)
H41F	0.378(2)	0.0002(7)	0.1989(5)	0.107(5)
H31F	0.840(2)	−0.0226(6)	0.2019(5)	0.081(4)
H31E	−0.0058(14)	0.5565(4)	0.5541(3)	0.018(2)
H3B	−0.169(2)	0.2678(7)	−0.0479(6)	0.100(4)
H6C	1.318(3)	0.7604(8)	0.5659(6)	0.125(5)
H71F	0.685(2)	0.1734(5)	0.0518(4)	0.054(3)
H21F	0.902(2)	0.0904(7)	0.1682(5)	0.097(4)
H01D	0.3032(17)	0.5379(5)	0.2979(4)	0.045(3)
H71D	0.6762(17)	0.6464(5)	0.2733(4)	0.041(3)
H21E	−0.3364(18)	0.5280(5)	0.5377(4)	0.051(3)

Table 9 (*continued*)

Atom	*x*	*y*	*z*	U_{iso} (Å^2)
H72D	0.417(2)	0.6641(6)	0.3038(5)	0.090(4)
H41E	−0.120(2)	0.4944(7)	0.4524(5)	0.104(4)
H32E	0.179(2)	0.4565(7)	0.5663(5)	0.075(4)
H73D	0.384(2)	0.6559(7)	0.2366(6)	0.094(4)
H41D	0.540(2)	0.4941(7)	0.1014(5)	0.092(4)
H31D	0.835(3)	0.5534(8)	0.1877(6)	0.127(5)
H4A	0.561(2)	0.1299(6)	0.2759(4)	0.065(3)
H51D	1.0640(17)	0.4179(5)	0.1237(4)	0.041(3)
H32F	0.350(2)	−0.0429(7)	0.1283(5)	0.099(4)
H42D	0.572(2)	0.4115(6)	0.1311(4)	0.067(3)
H32D	0.8644(19)	0.4686(6)	0.2171(4)	0.067(3)
H22F	0.590(3)	0.1033(8)	0.1462(6)	0.126(5)
H72E	−0.278(3)	0.6509(7)	0.5715(6)	0.108(5)
H72F	0.959(3)	0.1736(7)	0.0913(6)	0.100(5)
H52E	0.338(2)	0.5023(7)	0.4559(5)	0.112(5)
H82D	0.839(2)	0.3650(7)	0.0462(5)	0.092(4)
H73F	0.922(2)	0.1682(7)	0.0312(5)	0.091(4)
H83D	1.033(2)	0.4328(7)	0.0108(5)	0.101(4)
H52D	1.031(2)	0.5037(6)	0.0948(4)	0.073(4)
H82F	0.398(2)	−0.0820(7)	0.2925(6)	0.103(5)
H02C	−0.3931(18)	0.5350(5)	0.6379(4)	0.047(3)
H82E	0.350(2)	0.4109(6)	0.3651(5)	0.083(4)
H4C	1.159(3)	0.6046(8)	0.3743(6)	0.114(5)
H73E	0.004(3)	0.6552(7)	0.6194(6)	0.104(5)
H3A	0.190(3)	0.2794(8)	0.2899(6)	0.122(5)
H42E	−0.158(3)	0.4157(8)	0.4930(6)	0.142(5)
H83E	0.088(2)	0.3604(7)	0.3923(6)	0.106(5)
H3C	1.549(3)	0.7759(8)	0.3832(6)	0.131(5)
H83F	0.552(3)	−0.1745(9)	0.2916(6)	0.142(5)
H4B	0.239(3)	0.1184(8)	−0.0477(6)	0.123(5)
H22E	−0.396(3)	0.4576(9)	0.5718(6)	0.150(5)
H52F	0.579(3)	−0.1569(9)	0.2129(7)	0.152(6)

each other that the refinement of anisotropic displacement parameters was not sensible. These two substantially different conformations of the lysine molecules are clearly visible in the structure of the low-temperature phase.

We have obtained the following picture of these two conformations in phase I.

In the first conformation, the atoms C12–C13⋯C16–N12 that form the chain lie approximately in the same plane. In the second conformation, only atoms C23–C24–C25–C26 lie in the plane and bonds C26–N22 and C23–C22 form angles of approximately 110° with that plane.

Taking into account lysine molecules, only isotropic displacement parameters were refined in the incommensurate phase, in a similar way as in phase I.

All hydrogen atoms were added geometrically and their atomic parameters were not refined. Despite this idealisation, no further constraints were used during the refinement. The model of the structure of the incommensurate phase was constructed on the basis of the features present in its average structure and the superstructure of the low-temperature phase. Namely, it was assumed that occupation modulation is present for the lysine molecules, which accounts for the presence of two conformations. Moreover, displacive modulation functions were applied to both lysine and tartaric acid molecules. This type of modulation may be inferred from the low-temperature structure in which it is clearly visible that these molecules are displaced along the direction [101] of the unit cell.

Occupation and displacive modulation functions were applied to the molecules considered as rigid units using features of JANA2000. Only harmonic modulation functions were used in refinement, since only first-order satellites are visible in the incommensurate phase.

Refinement converged smoothly to the *R* factors of 6.84% for main reflections and 14.55% for first-order satellites. The refined parameters of the modulation functions reflect anticipated the character of the occupational waves, i.e. the amplitudes are approximately the same and close to one, but have opposite phases.

Vibrational spectra: Vibrational spectra of the polycrystalline sample of the normal and deuterated analogue of the studied crystal are shown in Figs. 10 and 11 and the bands observed are accumulated in Table 12, together with their assignments.

There is a carboxylic group of tartaric acid that is not ionised and vibrational spectra support this fact (see Table 12).

Vibrations of L*-lysine cations*: The strong shoulder at 3319 cm^{-1} and a very strong band at 3243 cm^{-1} in the infrared spectrum are attributed to stretching vibrations of NH_3 groups. Bands corresponding to scissoring, rocking and wagging types of vibrations for NH_3 group are observed at 1657 cm^{-1} (*R*, w), 1218 cm^{-1} (IR, s), 1225 cm^{-1} (*R*, vw), 1171 cm^{-1} (IR, s; *R*, vw) and 626 cm^{-1} (IR, m; *R*, vw), respectively. The problem concerning vibrations of NH_3 group is a little more complicated. The band at 493 cm^{-1} (IR, m; *R*, vw) is assigned as a combination band being the difference between scissoring and rocking types of vibrations of the above-discussed groups. It is rather difficult to distinguish the bands originating from the vibrations of NH_3 groups of L-lysine cations.

Hydrogen bonds vibrations: The stretching type of vibrations of hydrogen bonds gives rise to several bands in the region of 3250–2450 cm^{-1} (Table 12). The absorption bands at 1383 cm^{-1} (IR, vs), 1379 cm^{-1} (*R*, w), 1365 cm^{-1} (IR, vs; *R*, w), 1290 cm^{-1} (IR, s; *R*, w), 1266 cm^{-1} (IR, s) and 1254 cm^{-1} (IR, vs; *R*, vw) can arise from the O–H⋯O in-plane bending (δOH) type of vibrations of hydrogen bonds present in the studied crystal. Such an assignment is supported by the fact that in the case of Rochelle salt ($NaKC_4O_4H_6 \cdot 4H_2O$) the bands originating from δOH type of vibrations were observed at 1390 cm^{-1} and 1347 cm^{-1} [35]. The medium band observed at 812 cm^{-1} in the infrared spectrum only

Table 10
Anisotropic displacement parameters (Å^2) at 260 K

Atom	U^{11}	U^{22}	U^{33}	U^{12}	U^{13}	U^{23}
O1A	0.0181(3)	0.0498(4)	0.0326(4)	0.0032(3)	−0.0034(3)	0.0035(3)
O2A	0.0301(4)	0.0517(4)	0.0292(4)	0.0079(3)	−0.0020(3)	0.0055(4)
C1A	0.0287(5)	0.0299(5)	0.0248(5)	−0.0008(5)	−0.0002(5)	0.0000(5)
O3A	0.0318(4)	0.0417(4)	0.0341(4)	0.0018(3)	−0.0037(3)	0.0082(4)
C2A	0.0224(5)	0.0320(5)	0.0259(5)	0.0055(4)	−0.0001(4)	0.0014(5)
O4A	0.0527(5)	0.0380(4)	0.0378(4)	0.0058(3)	−0.0072(4)	0.0008(4)
C3A	0.0309(6)	0.0384(6)	0.0252(5)	−0.0004(5)	−0.0011(5)	−0.0010(5)
O5A	0.0415(4)	0.0669(5)	0.0256(4)	0.0077(4)	−0.0076(3)	−0.0120(4)
O6A	0.0536(5)	0.0637(5)	0.0475(5)	0.0074(4)	−0.0180(4)	−0.0233(4)
C4A	0.0334(6)	0.0365(6)	0.0333(6)	−0.0029(5)	−0.0008(5)	0.0049(5)
O1B	0.0333(4)	0.0464(4)	0.0251(4)	0.0022(3)	0.0003(3)	0.0049(3)
O2B	0.0224(4)	0.0572(4)	0.0343(4)	0.0026(4)	−0.0033(3)	0.0023(4)
C1B	0.0291(5)	0.0296(5)	0.0276(5)	−0.0010(5)	−0.0056(5)	−0.0012(5)
O3B	0.0333(4)	0.0377(4)	0.0342(4)	−0.0052(3)	−0.0053(3)	0.0068(3)
C2B	0.0246(5)	0.0284(5)	0.0243(5)	0.0014(4)	−0.0064(4)	−0.0008(5)
O4B	0.0442(4)	0.0396(4)	0.0390(4)	0.0071(3)	−0.0040(4)	−0.0064(4)
C3B	0.0348(6)	0.0386(6)	0.0292(6)	−0.0027(5)	0.0013(5)	0.0022(5)
O5B	0.0367(4)	0.0690(5)	0.0312(4)	0.0091(4)	−0.0038(4)	−0.0052(4)
O6B	0.0422(4)	0.0608(5)	0.0376(4)	0.0012(4)	−0.0154(4)	−0.0160(4)
C4B	0.0377(6)	0.0397(6)	0.0237(6)	−0.0032(5)	−0.0015(5)	0.0101(5)
O1C	0.0232(4)	0.0520(4)	0.0331(4)	−0.0032(4)	−0.0041(3)	0.0006(3)
O2C	0.0316(4)	0.0450(4)	0.0267(4)	0.0026(3)	0.0006(3)	−0.0033(3)
C1C	0.0242(5)	0.0305(5)	0.0287(5)	0.0011(5)	−0.0030(4)	0.0032(5)
O3C	0.0278(4)	0.0398(4)	0.0403(4)	−0.0049(3)	−0.0047(3)	−0.0037(3)
C2C	0.0314(6)	0.0372(6)	0.0273(6)	−0.0029(5)	−0.0035(5)	−0.0023(5)
O4C	0.0686(5)	0.0361(4)	0.0351(4)	−0.0025(3)	−0.0042(4)	0.0044(4)
C3C	0.0432(7)	0.0404(6)	0.0283(6)	−0.0009(5)	−0.0009(5)	−0.0033(6)
O5C	0.0796(6)	0.0589(5)	0.0465(5)	−0.0073(4)	−0.0252(4)	0.0202(5)
O6C	0.0471(5)	0.0922(6)	0.0318(4)	−0.0159(4)	−0.0050(4)	0.0128(5)
C4C	0.0365(6)	0.0502(7)	0.0280(6)	0.0050(5)	−0.0074(5)	−0.0025(6)
O1D	0.0338(4)	0.0527(4)	0.0468(4)	−0.0016(4)	−0.0111(4)	−0.0051(4)
O2D	0.0443(4)	0.0423(4)	0.0466(4)	0.0049(4)	−0.0080(4)	0.0041(4)
C1D	0.0279(5)	0.0359(6)	0.0353(6)	−0.0021(5)	−0.0003(5)	0.0048(5)
C0D	0.0307(5)	0.0391(6)	0.0326(6)	−0.0080(5)	−0.0083(5)	0.0072(5)
N1D	0.0350(5)	0.0317(5)	0.0441(5)	−0.0044(4)	−0.0063(4)	0.0023(4)
C2D	0.0278(5)	0.0408(6)	0.0330(6)	−0.0032(5)	−0.0018(5)	0.0016(5)
C3D	0.0401(6)	0.0468(7)	0.0326(6)	−0.0077(5)	−0.0030(5)	−0.0021(6)
C4D	0.0395(6)	0.0432(7)	0.0387(6)	−0.0017(6)	−0.0056(5)	−0.0038(6)
C5D	0.0403(6)	0.0568(7)	0.0350(6)	−0.0111(6)	−0.0054(5)	0.0019(6)
N2D	0.0418(5)	0.0433(5)	0.0386(5)	−0.0079(4)	−0.0095(4)	0.0048(5)
O1E	0.0469(4)	0.0387(4)	0.0524(5)	0.0094(4)	−0.0069(4)	−0.0002(4)
O2E	0.0308(4)	0.0509(4)	0.0588(5)	−0.0078(4)	−0.0119(4)	−0.0031(4)
C1E	0.0313(6)	0.0406(6)	0.0316(6)	−0.0057(5)	0.0027(5)	0.0033(5)
C0E	0.0364(6)	0.0317(6)	0.0454(7)	−0.0032(5)	−0.0115(5)	0.0004(5)
N1E	0.0498(6)	0.0402(5)	0.0493(6)	−0.0107(5)	−0.0128(5)	0.0052(5)
C2E	0.0501(7)	0.0709(8)	0.0448(7)	−0.0167(6)	−0.0132(6)	0.0081(7)
C3E	0.0433(6)	0.0811(9)	0.0326(6)	−0.0044(6)	−0.0006(6)	0.0141(7)
C4E	0.0574(8)	0.0796(9)	0.0461(7)	−0.0061(7)	0.0016(6)	0.0176(7)
C5E	0.0592(8)	0.1115(10)	0.0419(7)	−0.0222(8)	−0.0073(6)	−0.0179(8)
N2E	0.0364(5)	0.0503(6)	0.0331(5)	−0.0076(4)	−0.0041(4)	0.0027(5)
O1F	0.0341(4)	0.0543(5)	0.0605(5)	0.0076(4)	−0.0129(4)	0.0021(4)
O2F	0.0509(4)	0.0407(4)	0.0514(5)	−0.0078(4)	−0.0080(4)	0.0037(4)
C1F	0.0302(6)	0.0397(6)	0.0387(6)	0.0077(5)	−0.0028(5)	−0.0035(5)
C0F	0.0309(6)	0.0313(6)	0.0314(6)	0.0044(5)	−0.0020(5)	−0.0079(5)
N1F	0.0342(5)	0.0384(5)	0.0451(5)	0.0100(4)	−0.0072(4)	−0.0044(4)
C2F	0.0666(7)	0.0357(6)	0.0318(6)	0.0052(5)	0.0086(6)	−0.0109(6)
C3F	0.0497(7)	0.0382(6)	0.0466(7)	0.0087(5)	0.0019(6)	−0.0133(6)
C4F	0.0502(7)	0.0527(7)	0.0545(7)	0.0172(6)	−0.0066(6)	−0.0092(6)
C5F	0.0568(7)	0.0502(7)	0.0391(7)	0.0115(6)	−0.0025(6)	−0.0142(6)
N2F	0.0438(5)	0.0338(5)	0.0414(5)	0.0004(4)	−0.0029(5)	−0.0040(4)

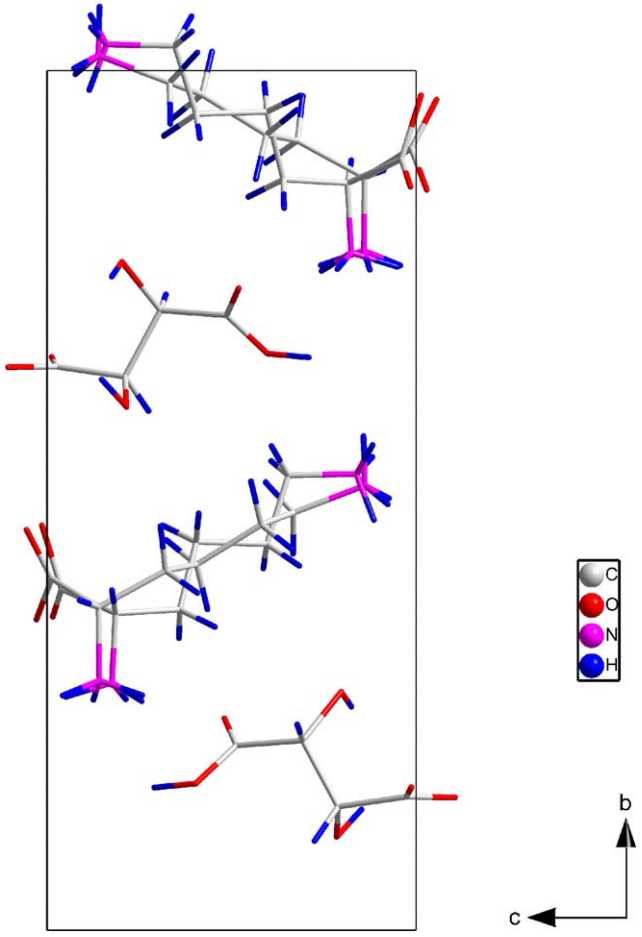

Fig. 1. Unit cell of phase I at 320 K.

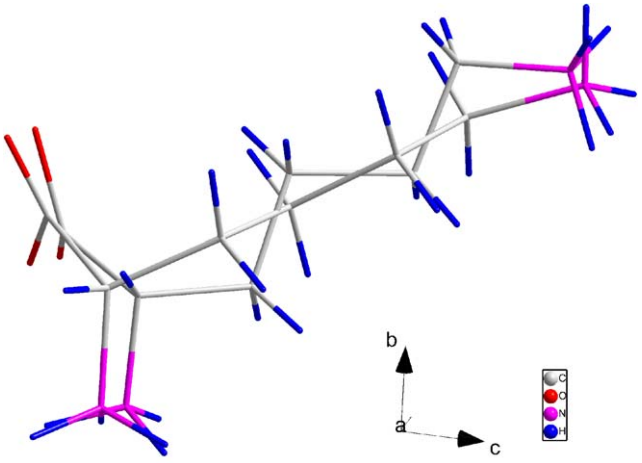

Fig. 2. Details of the unit cell of phase I at 320 K—disordered lysine molecules.

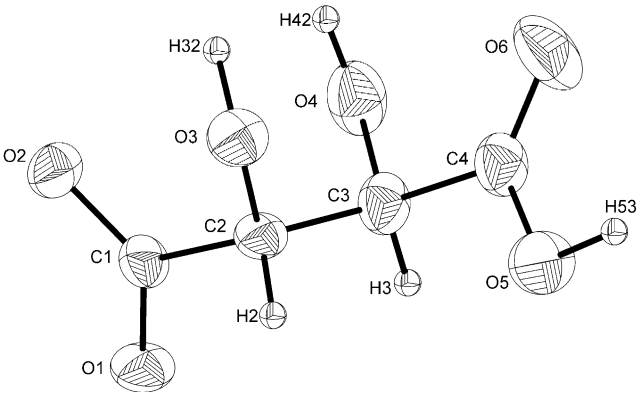

Fig. 3. Atom names of tartaric acid molecule and anisotropic displacement parameters at 320 K.

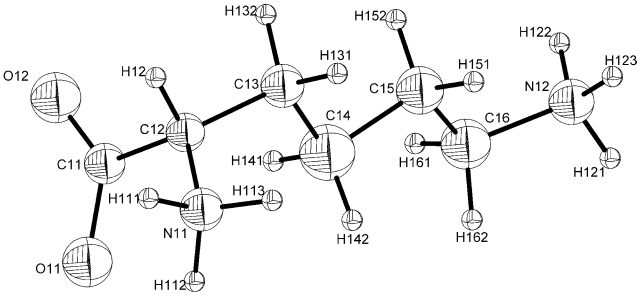

Fig. 4. Atom names of lysine molecule (conformation 1) and isotropic displacement parameters at 320 K.

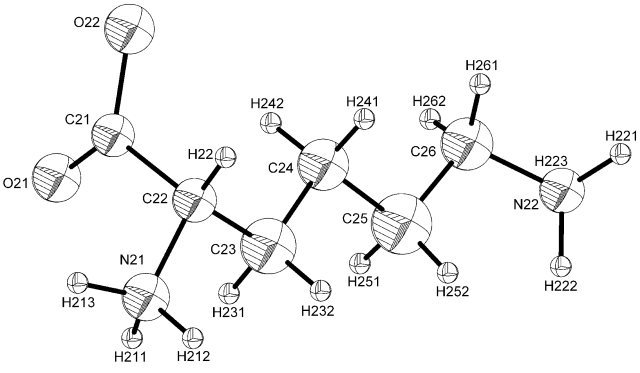

Fig. 5. Atom names of lysine molecule (conformation 2) and isotropic displacement parameters at 320 K.

was assigned to the O–H···O out-of-plane bending (γOH) type of vibrations of hydrogen bonds. The analogous band corresponding to this type of vibration for N–H···O hydrogen bond was found at 937 cm^{-1} (IR, m; *R*, vw). The strong and broad absorption centred at approximately 1200 cm^{-1} corresponds to the presence of strong hydrogen bonds with approximately 2.54 Å length.

Phase transitions: DSC measurements on the powder samples indicate two-phase transition points at about

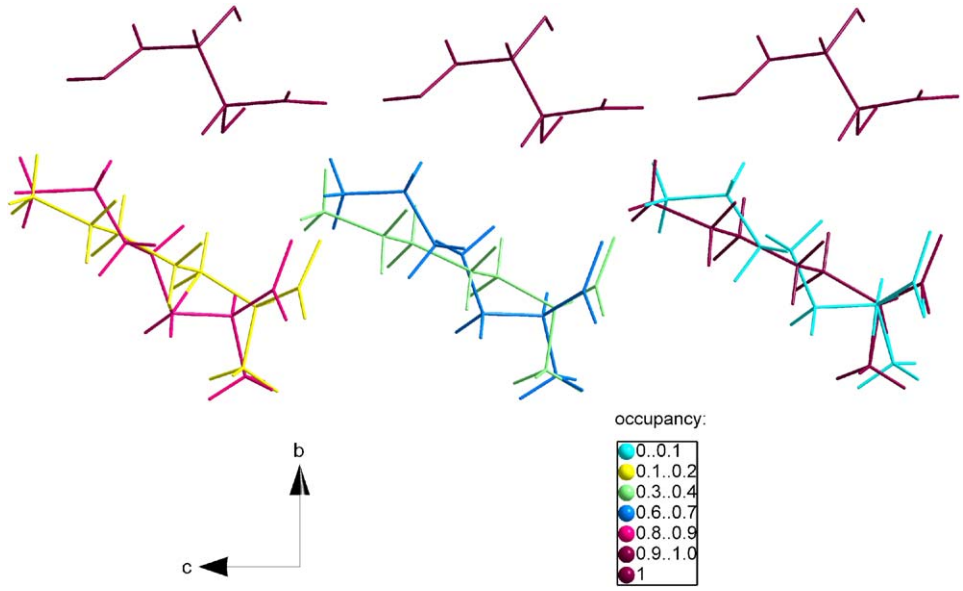

Fig. 6. Incommensurate phase at 298 K. Model of the crystal exhibiting displacive and occupation modulation waves.

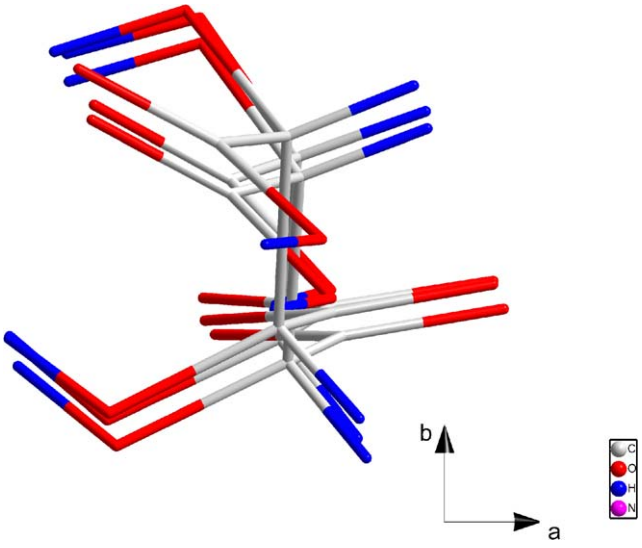

Fig. 7. Incommensurate phase at 298 K. Example of the displacive modulation of tartaric acid molecule.

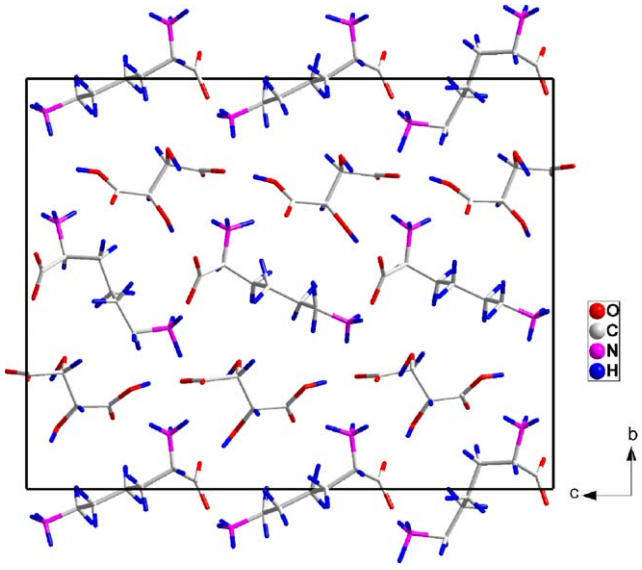

Fig. 8. Unit cell of phase III at 260 K.

295, 300 and 293, 300 K for heating and cooling, respectively (Fig. 12).

Also, temperature dependencies of the lattice parameters show anomalies in the vicinity of room temperature (Fig. 13(a–d)). Phase I, existing above ~303 K, has a monoclinic unit cell with parameters at 320 K presented in Table 1. The lattice parameters a, b, and c depicted in Fig. 13 (a–d) are multiplied by 3. With decreasing temperature additional reflexes appear in between main reflexes along the c^* direction. This indicates a new phase II which is stable in the temperature range of 303–295 K. Phase II can be described as a incommensurate modulated one with modulation vector $q = \alpha\mathbf{a}^*(1/3 + d)c^*$. Below ca. 295 K, d-parameter becomes zero and a new phase III shows commensurate modulation with modulation vector $q = 1/3c^*$—it means that the super cell of the phase III is three times expanded in the crystallographic z direction in comparison with the unit cell of phase I. Nevertheless, the crystal remains monoclinic at the 320–260 K temperature range.

SHG experiment: For the powder second harmonic generation efficiency of the crystal presented here we have obtained the following value relative to KDP: $d_{eff} = 0.35\ d_{eff}$ (KDP).

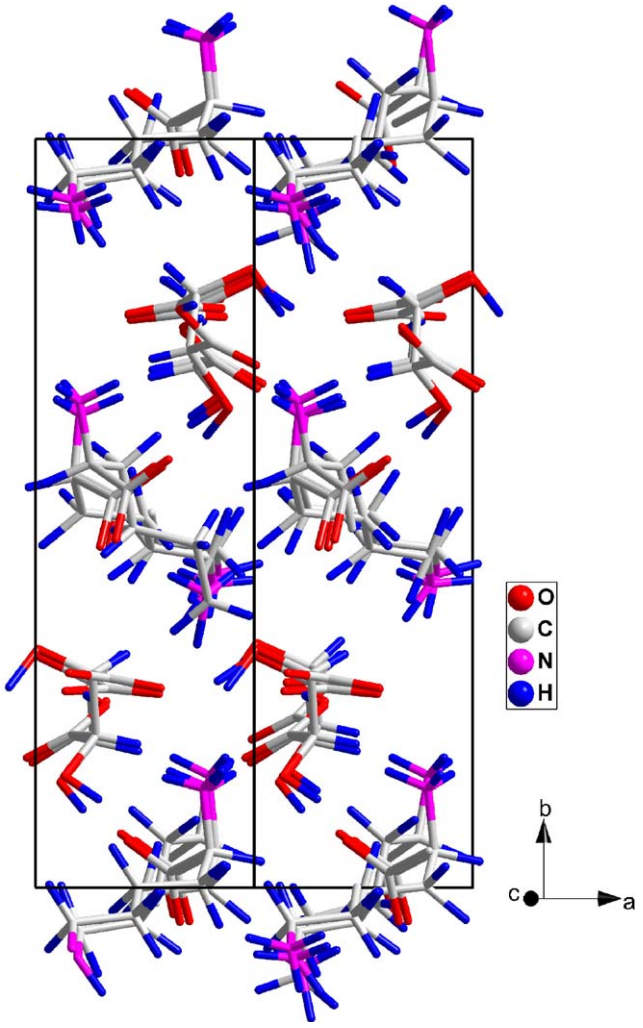

Fig. 9. Projection of the unit cell of phase III at 260 K along the direction (101).

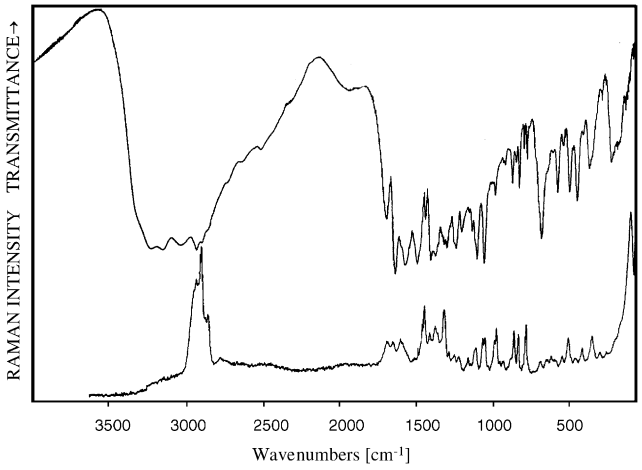

Fig. 10. FTIR and FTRaman room-temperature powder spectra of L-lysine-L-tartaric acid crystal.

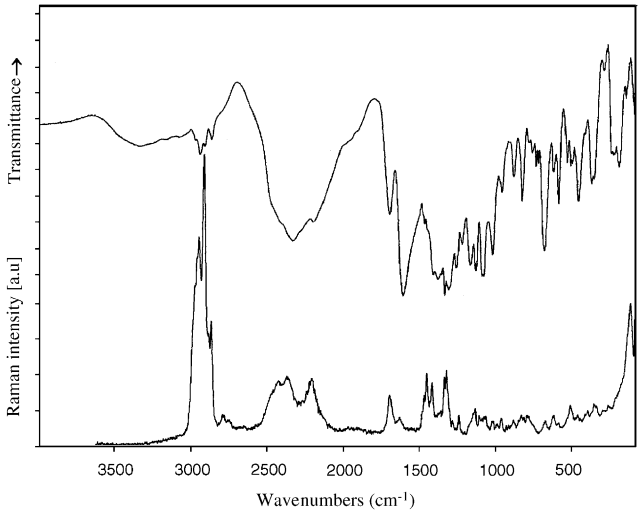

Fig. 11. FTIR and FTRaman room-temperature powder spectra of deuterated L-lysine-L-tartaric acid crystal.

Table 11
Hydrogen-bonds for L-lysine-L-tartaric acid at 320 K

D–H···A	D–H (Å)	H···A (Å)	D···A (Å)	Angle D–H···A (deg)
O(1D)–H(1D)···O(2A)#5	1.017(16)	1.534(16)	2.5419(11)	170.0(19)
O(1B)–H(2B)···O(1A)#3	0.974(11)	1.830(11)	2.7377(11)	153.9(10)
O(1C)–H(2C)···O(1B)	1.162(16)	2.154(16)	3.0125(11)	128.1(11)
N(1)–H(1A)···O(2A)#7	0.849(15)	2.034(15)	2.8482(12)	160.6(14)
N(1)–H(1C)···O(2)#2	0.969(18)	1.975(17)	2.8625(14)	151.2(14)
N(2)–H(2B)···O(1A)#5	0.899(14)	2.382(13)	2.8281(12)	110.8(10)
N(2)–H(2B)···O(1)	0.899(14)	2.412(14)	2.7022(13)	99.0(10)
N(2)–H(2A)···O(2D)#1	1.021(15)	1.849(14)	2.8385(14)	162.3(12)
N(2)–H(2C)···O(1C)#8	0.942(13)	2.188(12)	3.0329(15)	148.8(12)

Symmetry transformations used to generate equivalent atoms: #1 $x+1,y,z$ #2 $x,y,z-1$ #3 $x-1,y,z$ #4 $-x+1,y-1/2,-z+1$. #5 $x,y,z+1$ #6 $-x+1,y+1/2,-z+1$ #7 $-x,y+1/2,-z$. #8 $x+1,y,z+1$.

Table 12
Wavenumbers (cm^{-1}) and relative intensities of the bands observed in the powder infrared and Raman spectra of L-lysine-L-tartaric acid and its deuterated analogue

		Deuterated		Assignment
FTIR	FTRaman	FTIR	FTRaman	
3319ssh		3334wb		Asymmetric stretching (NH_2 and NH_3)
3243vs				Symmetric stretching (NH_2 and NH_3) and O–H stretching
3167vs		3165wb		O–H stretching (for deuterated analogue: residual, non-deuterated part of crystal)
3049vs				O–H stretching
			2986msh	
		2971w	2975s	
	2961m		2960s	
2945vs	2948m	2943w	2948s	C–H asymmetric stretching
2910vs	2916s	2911w	2916vs	C–H symmetric stretching
	2884m		2888m	
2870ssh	2870m	2867w	2868m	O–H stretching (for deuterated analogue: residual, non-deuterated part of crystal)
2740m			2748vw	
2665m	2680vw			O–H stretching
2528m				
		2461s	2462wsh	O–D stretching
		2426s	2428w	O–D stretching
		2365s	2368w	O–D stretching
		2345s		
		2207m	2208w	O–D stretching
		1997w		
		1952w		
1940w				
		1910w		
1705s	1693w	1701s	1697vw	C=O stretching
1648vs	1657w			Scissoring (σ), (NH_2 and NH_3) and $\delta_a NH_3^+$
1607vwsh	1608w	1606vs		COO^- asymmetric stretching
1582vs				COO^- asymmetric stretching
1503vs	1495w			$\delta_s NH_3^+$
	1465w	1468s	1467w	
1449s		1452s	1453w	CH_2 scissoring (σ)
1415vs	1415w	1411s	1415w	COO^- symmetric stretching
1383vs	1379w	1379s		C–O stretching + O–H in-plane bending (δ) and COO^- symmetric stretching
1365vs	1364w	1359s		C–O stretching + O–H in-plane bending (δ)
1344s		1338vs	1338w	CH_2 twisting (τ)
1328s	1324m	1320vssh	1324w	CH_2 twisting (τ)
1310s	1316msh	1310vs		CH_2 twisting (τ)
1290s	1291w	1298vs	1281vw	C–O stretching + O–H in-plane bending (δ)
1266s				O–H in-plane bending (δ)
1254vs	1255vw	1259s		C–O stretching + O–H in-plane bending (δ)
1218s	1225vw	1221s		Rocking (ρ), (NH_2 and NH_3)
1171s	1170vw	1168s		Rocking (ρ), (NH_2 and NH_3)
1153s	1154vw	1162s		Rocking (ρ), (NH_2 and NH_3)
1135ssh	1131w	1131s	1133vw	Rocking (ρ), (NH_2 and NH_3)
1121vs	1122w			Rocking (ρ), (NH_2 and NH_3)
		1090s		
1077vs	1079w	1078s		C–N stretching
	1065w			
1046ssh				
1002s	1000w	1022s	1020vw	C–C stretching
	963vw	961m	963vw	
945m				N–H···O out-of-plane bending, (γ)
937m	936vw	930w		N–H···O out-of-plane bending, (γ)
889m	891vw	881w	881vw	C–C stretching
865m	871w			O–H···O out-of-plane bending (γ)
845s	842w			O–H···O out-of-plane bending (γ)
		828m	831vw	
812m				O–H···O out-of-plane bending (γ)
792m	792m	788w	794vw	
777w		781w		CH_2 rocking (ρ)
		762w		

Table 12 (*continued*)

		Deuterated		Assignment
FTIR	FTRaman	FTIR	FTRaman	
739msh		737w		CH_2 rocking (ρ)
720ssh		720w		
701s	695vw	680s	673vw	COO^- scissoring (σ)
664msh	657vw			
	648vw			
625m	627vw	621w	621vw	NH_2 wagging (ωNH_2)
593s	602vw	586m	584vw	COO^- wagging (ω)
553m	552vw			
		533w		
516m	515w	502w	510w	N···O stretching
493m	494vw			Scissoring–rocking, (NH_2 and NH_3)
463s	465vw	456m	460vw	
427w	420w	416w		
			395vw	
385m				δ(skel.)
369msh		371m		skel. def. and τ(C–C), lattice
	357w	354m	354w	
304w	302w			
259msh	264w		258vw	δ(skel.)
244m				δ(skel.)
		228w		
197m		191w		τ COO^-
147w		144vw		Lattice
			129msh	Lattice
	117s		115m	Lattice
		91vw		Lattice
	83vs			Lattice

S, strong; w, weak; v, very; sh, shoulder; b, broad; m, medium.

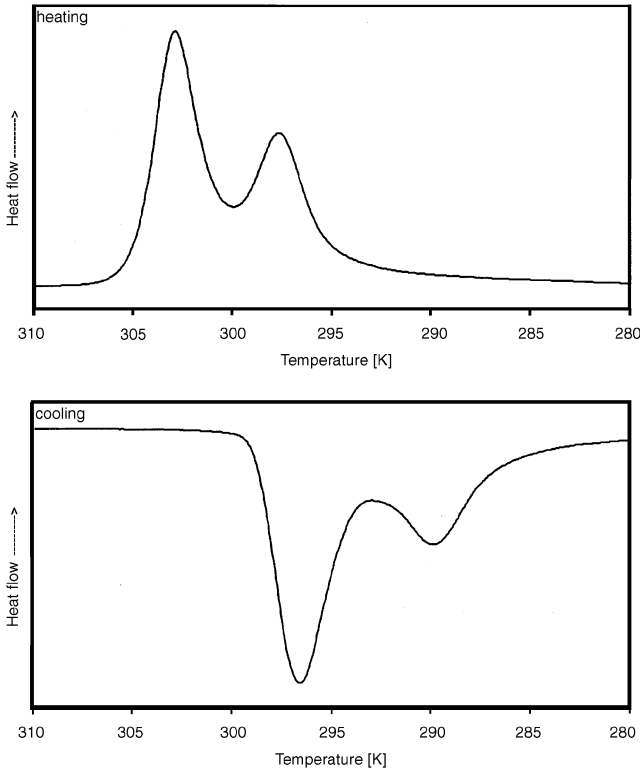

Fig. 12. DSC diagrams for L-lysine-L-tartaric acid.

4. Summary

Vibrational spectra support structural data. Similar to recently studied [55] rubidium hydrogen tartrate, due to non-centrosymmetric structure, L-lysine-L-tartaric acid can possess potential application as a optically nonlinear crystal.

In the normal phase ($P2_1$ space group) above ca. 303 K the crystal structure has been determined at 320 K for the following lattice parameters $a = 5.104$ Å, $b = 17.525$ Å and $c = 7.588$ Å, with $\beta = 97.60^\circ$. In the incommensurate phase with $\mathbf{q} = \alpha\mathbf{a}^* + \gamma\mathbf{c}^*$ (301–296 K) the average structure has been calculated for unit cell with the lattice parameters: $a = 5.103$ Å, $b = 17.445$ Å and $c = 7.538$ Å with $\beta = 97.94^\circ$, and amplitudes of the displacive and occupation modulation waves were refined. In the low-temperature phase with the commensurate modulated vector $\mathbf{q} = 1/3\mathbf{c}^*$ (296–150 K) the data were collected at 260 K and the crystal structure was solved for monoclinic system with a $P2_1$ space group with the following lattice parameters: $a = 5.124$ Å, $b = 17.385$ Å and $c = 22.400$ Å with $\beta = 95.08^\circ$.

The recording of vibrational spectra as a function of temperature (350–14 K) will be the subject of the further studies. Spectra and details of data collection and

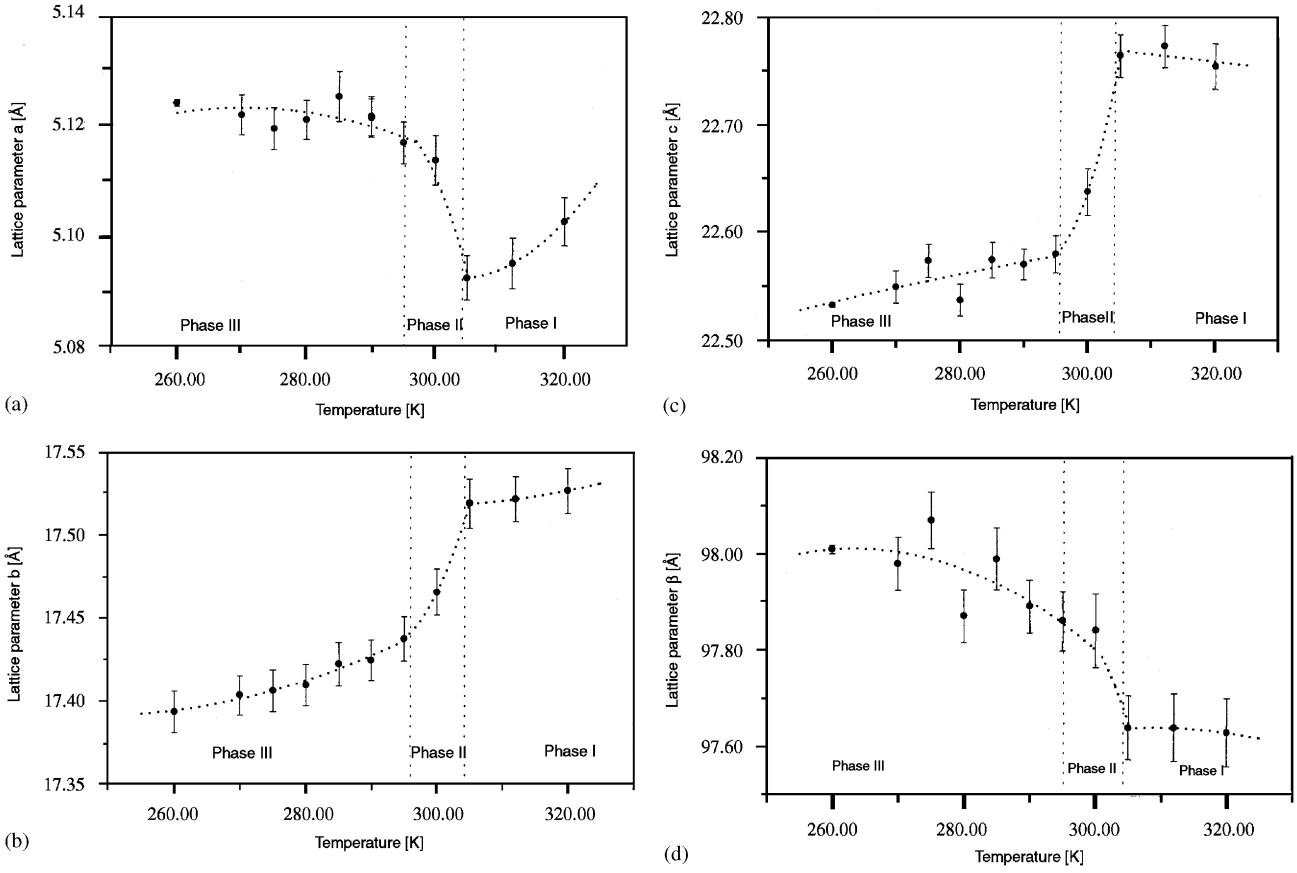

Fig. 13. Lattice parameters temperature dependencies of L-lysine-L-tartaric acid crystal (eyes guide marked by dotted line): (a) lattice parameter a, (b) lattice parameter b, (c) lattice parameter c and (d) monoclinic angle β.

refinement for low-temperature phase III will be given in a separate paper.

Acknowledgments

This work was financially supported by the Polish Ministry of Scientific Research and Information Technology (Project no. T09A 121 28).

References

[1] A. Pietraszko, M. Marchewka, A. Haznar, M. Drozd, Crystal strurcture and phase transitions in a new compound: L-lysine-L-tartaric acid, XXV International School and IV Polish–Ukrainian Ferroelectric Physics Meeting, 18–22 September, 2000, Crakow, Poland.
[2] F. Stern, C.A. Beevers, Acta Crystallogr. 3 (1950) 341.
[3] Y. Okaya, N.R. Stemple, M.I. Kay, Acta Crystallogr. 21 (1966) 237.
[4] D. Braga, A. Angeloni, E. Tagliavini, F. Grepioni, J. Chem. Soc. Dalton Trans. 12 (1998) 1961.
[5] E. Weber, N. Dorpinghaus, C. Wimmer, Z. Stein, H. Krupitsky, I. Goldberg, J. Org. Chem. 57 (1992) 6825.
[6] B. Gunes, H. Soylu, Acta Crystallogr. C 51 (1995) 2346.
[7] H. Soylu, Z. Kristallogr. 171 (1985) 255.
[8] M. Akkurt, T. Hokelek, H. Soylu, Z. Kristallogr. 181 (1987) 161.
[9] V.S. Yadawa, V.M. Padmanabhan, Acta Crystallogr. B 29 (1973) 493.
[10] G.K. Ambady, G. Kartha, Acta Crystallogr. B 24 (1968) 1540.
[11] G.K. Ambady, Acta Crystallogr. B 24 (1968) 1548.
[12] U. Rychlewska, B. Warzajtis, M. Hoffmann, J. Rychlewski, Molecules 2 (1997) 106.
[13] J. Kivikoski, J. Vepsalainen, R. Suontamo, E. Pohjala, R. Laatikainen, Tetrahedron-Asymmetry 4 (1993) 709.
[14] T. Koritsanszky, D. Zobel, P. Luger, J. Phys. Chem. 104 (2000) 1549.
[15] M. Akkurt, I. Celik, S. Ozbey, E. Kendi, Z. Kristallogr. 215 (2000) 71.
[16] A.N. Chekhlov, I.V. Martynov, Dokl. Akad. Nauk 365 (1999) 492 (in Russian).
[17] P. Starynowicz, G. Meyer, Z. Anorg. Allg. Chem. 626 (2000) 2441.
[18] U. Rychlewska, B. Warzajtis, Acta Crystallogr. B 56 (2000) 833.
[19] G.P. Srivastava, S. Mohan, Y.S. Jain, J. Raman Spectrosc. 13 (1982) 25.
[20] N. Kaneko, M. Kaneko, H. Takahashi, Spectrochim. Acta 40A (1984) 33.
[21] V. Ramakrishnan, J.M.T. Maroor, Infrared Phys. 28 (1988) 201.
[22] P. Rajagopal, G. Sekar, G. Aruldhas, V. Ramakrishnan, Proc. Indian Acad. Sci. Chem. Sci. 101 (1989) 243.
[23] Chen Zhan, H.L. Strauss, J. Chem. Phys. 108 (1998) 5522.

[24] P.L. Polavarapu, C.S. Ewig, T. Chandramouly, J. Am. Chem. Soc. 109 (1987) 7382.
[25] M. Koralewski, M. Szafranski, Ferroelectrics 80 (1988) 917.
[26] M. Koralewski, M. Szafranski, Ferroelectrics 97 (1989) 233.
[27] M. Szafranski, Ferroelectrics 129 (1992) 55.
[28] T. Tsukamoto, H. Futame, Phase Trans. 45 (1993) 59.
[29] M. Maeda, K. Honda, I. Suzuki, J. Phys. Soc. Jpn. 7 (1995) 2642.
[30] K. Deguchi, Y. Iwata, J. Phys. Soc. Jpn. 1 (2000) 135.
[31] B. Gerth, A. Sahling, G. Pompe, E. Hegenbarth, B. Brezina, Phys. Stat. Sol. (A) 57 (1980) K153.
[32] M.M. Abdelkader, Z.H. Eltanahy, M. Abutaleb, A. Abousehly, A. Elsharkawy, Philos. Mag. B 72 (1995) 91.
[33] K.E. Haller, Proceedings of the Tenth International Conference on Raman Spectroscopy, Raman 86, Eugene, University of Oregon, 1986, pp. 11/17–18, Eugene, OR, USA.
[34] I. Kanesaka, H. Kita, J. Raman Spectrosc. 23 (1992) 585.
[35] P. Kolandaivel, S. Selvasekarapandian, Cryst. Res. Tech. 28 (1993) 665.
[36] I. Kanesaka, N. Kita, J. Raman Spectrosc. 27 (1996) 811.
[37] S. Kamba, B. Brezina, J. Petzelt, G. Schaack, J. Phys.: Condens. Matter 8 (1996) 8669.
[38] S. Kamba, G. Schaack, J. Petzelt, B. Brezina, J. Phys.: Condens. Matter 8 (1996) 4631.
[39] S. Kamba, G. Schaack, J. Petzelt, B. Brezina, Ferroelectrics 186 (1996) 181.
[40] S. Kamba, G. Schaack, J. Petzelt, Phys. Rev. B 51 (1995) 14998.
[41] H. Ratajczak, Proceedings of the Third International Conference, "Vibrational Spectroscopy in Materials Science", 23–26 September 2000, Krakow, Poland, Book of Abstracts, p. 21.
[42] H. Ratajczak, Proceedings of the Third International Conference, "Vibrational Spectroscopy in Materials Science", 23–26 September 2000, Krakow, Poland, Book of Abstracts, p. 31.
[43] H. Ratajczak, Proceedings of the Third International Conference, "Vibrational Spectroscopy in Materials Science", 23–26 September 2000, Krakow, Poland, Book of Abstracts, p. 59.
[44] J. Fuller, Acta Crystallogr. C 51 (1995) 1680.
[45] T.N.G. Row, Coordination Chem. Rev. 183 (1999) 81.
[46] M. Oussaid, M. Kemiche, P. Becker, C. Carabatos-Nedelec, O. Watanabe, Phys. Stat. Sol. (B) 196 (1996) 487.
[47] P. Dastidar, T.N.G. Row, B.R. Prasad, C.K. Subramanian, S. Bhattacharya, J. Chem. Soc. Perkin Trans. 2 (1993) 2419.
[48] N. Blagden, K.R. Seddon, Cryst. Eng. 2 (1999) 9.
[49] A. Padnan, C.C. Becerra, J. Phys.: Condens. Matter 12 (2000) 2071.
[50] KUMA Diffraction, KM4/CCD Users' Guide, Version 1.169 (Release April, 2000), Wrocław, Poland.
[51] G.M. Sheldrick, SHELXL, Program for Crystal Structure Refinement, University of Goettingen, Germany, 1993.
[52] M. Sheldrick, SHELXL, Program for Crystal Structure Refinement, University of Goettingen, Germany, 1997.
[53] S.K. Kurtz, T.T. Perry, J. Appl. Phys. 39 (1968) 3798.
[54] F.H. Allen, O. Kennard, D.G. Watson, L. Brammer, A.G. Orpen, R. Taylor, J. Chem. Soc. Perkin Trans. 2 (1987) S1–S19.
[55] M. Ben Salah, K. Mouaine, P. Becker, C. Carabatos-Nedelec, Phys. Stat. Sol. (B) 220 (2000) 1025.
[56] V. Petricek, M. Dusek, L. Palatinus, JANA2000. The crystallographic computing system, Institute of Physics, Praha, Czech Republic, 2000.
[57] A. Schönleber, M. Meyer, G. Chapuis, J. Appl. Crystallogr. 34 (2001) 777.
[58] T. Janssen, A. Janner, A. Looijenga-Vos, P.M. de Wolff, International Tables for Crystallography, vol. C, Kluwer, Dodrecht, 1995, p. 797.